

## Original Article



# Effects of Fourier Transform and Modal Theory on Cable Fault Location

Mojtaba Sedghi Amiri<sup>1</sup> | Ebadollah Amouzad Mahdiraji<sup>2\*</sup> <sup>1</sup> Neka Power Generation Management Company, Mazandaran, Iran<sup>2</sup> Department of Engineering, Sari Branch, Islamic Azad University, Sari, Iran

**Citation** M.S. Amiri, E.A. Mahdiraji, **Effects of Fourier Transform and Modal Theory on Cable Fault Location**, *Eurasian J. Sci. Technol.*, 2021, 1(1), 11-19.

<https://doi.org/10.48309/ejst.2021.130258>

**Article info:**

Received: 04 January 2021

Accepted: 30 April 2021

Available Online: 05 May 2021

ID: JSTR-2104-1006

Checked for Plagiarism: Yes

Checked for language: Yes

**Keywords:**

Fault detection and localization indicators, Power cables, Short circuit fault, Fourier transform, Clarke transform, Modal components.

**ABSTRACT**

One of the most commonly used equipment in the power system, which is exposed to various types of faults for various reasons, is high and low voltage pressure cables. Due to the fact that cables, either power or distribution cables are mostly transported from underground, despite their further reliability in airway, they are more difficult to repair and possibly replace in case of fault, in line with this the correct fault detection and location of them is of utmost important. In this paper, as is clear from the title of the research, the Fourier transform and Modal transform methods are used to find the type and location of faults, so that the efficiency of the selected method for detecting and locating the faults in underground transmission cables is examined and the speed and accuracy of finding a solution to the problem is assessed. In this paper, it is expected that the Fourier transform method, followed by the Modal transform has substantial speed and accuracy in determining the type and location of the faults. Meanwhile, the detection and location indicators are used to determine the type and location of the fault, which as shown in the simulations, will have efficient performance. The sample model is simulated to demonstrate the correctness of these methods. The simulation results from MATLAB and EMTP/ATP software confirm the precise and rapid performance of the proposed method.

**Introduction**

In ANSI/IEEE Std.100-1992 standard fault is defined as a physical condition that results in the failure of a device, a component, or an element to perform a necessary routine. A short or definitive wire termination includes this definition. A fault almost always involves a short circuit between electric phase conductors or between a phase and ground. The fault may be a screw connection or may have some impedance at the

fault location. The term “fault” which is used as the “short circuit” synonym is defined in the abovementioned standards [1]. Due to the defects that occur in ground cables, the type of methods used to determine the location of defects will also be different. So, firstly, the kind of defect which has appeared in the cable should be determined [2]. Generally, methods for determining the location of faults for cables, are divided into online and offline methods. In offline method, special tools are used to test the cable failure while in the online method; the

\*Corresponding Author: Ebadollah Amouzad Mahdiraji ([Ebad.Amouzad@gmail.com](mailto:Ebad.Amouzad@gmail.com))

voltage and current are sampled and processed to determine the fault point [3-7]. A location algorithm based on the two ends of cable is presented especially for the life-long power cables. The aging process in cable causes a change in the relative passivity coefficient and consequently leads to a change in capacitance of the positive, negative and zero capacitors. The fault location design is based on the measurement of Phasors from both ends of the cable in combination with the linear distribution model; Clarke transform and Discrete Fourier Transform Theory (DFT) [8]. In the reference [9] which differs from impedance-based methods, a repeatable algorithm is proposed for fault localization in cable. The circuit is modeled by distributed parameter method and the voltage and the current equations are formulated based on the sequential networks. The Newton-Raphson method is used to calculate the fault distance. The algorithm also extends to radial multi-section cables with light loads. Other works which have been implemented in exploiting the Allindar Dutch Network are presented in [10], [1]. Fault locators use only the calculated reactance. Since the fault impedance reactance is zero and the cable reactance is also specified and is not dependent on the current, short circuit scenarios are simulated in all nodes in a faulty feeder in a real network model. The calculated impedance is compared with the simulated impedance to find the exact location. This algorithm finds the distance location within 5 minutes after the occurrence of the fault. Another valid way of mobile waves is by changing the energy stored in the capacitor and inductor, which is produced on the lines or cables after the fault occurs. Both the voltage and the current waves propagate along the circuit at a velocity to that of a light, so as to encounter the impedance discontinuities, and then high frequency waves emanating from the fault are reflected and transferred to the other. Almost all the methods based on mobile waves follow the principle of Boolean diagram [12] and the fault distance is obtained by the product of the propagation velocity and the time interval of the fault which is equal to the time difference between the instant of the initial arrival of the wave-front and the moment

the wave-front is reflected. Principles of the basic locating and a variety of convention locating methods are introduced in [1].

In this paper, a 230 kV transmission network along with two sources at the two ends of the line (representing a power network on both sides) was first simulated in EMTP/ATP transient states software and then using the MATLAB software, time outputs of this software are transmitted via transmitting the Fourier transform to Phasor domain. Finally, using the detection and fault localization indicators, the type and location of the faults are recognized. The simulation results are presented in different figures and tables for several fault samples and different times with different fault resistances.

#### Fourier Transform

In general, Discrete Fourier Transform (DFT) is defined as follows [14]:

$$X(\omega) = \sum_{n=-\infty}^{\infty} x[n]e^{-i\omega n} \quad (1)$$

The above relation is considered as the main definition of the Fourier transform which is expressed in terms of discrete signals. If a signal is in a continuous form of  $x(t)$ , in order to obtain a discrete Fourier transform, first a discrete signal  $x'(k\Delta t)$  is considered which includes  $N$  sample of the sampled signal  $x(t)$ , the amount of which is expresses over time in relation (2):

$$x'(k\Delta T) = x(t)w(t) \sum_{k=-\infty}^{+\infty} \delta(t - k\Delta T) \quad (2)$$

Where  $\Delta T$  is the sampling period and  $w(t)$  is the function that contains  $N$  sample of the sampled signal of  $x(t)$  at the time interval  $T_0$ , that is, this function can be introduced as a function with the sampling window to  $N$  length. For stable applications, the length of the sampling window is constant but this window moves forward over time and the samples from  $-\infty$  to  $\infty$  enter and exit from the window, respectively and thus the sampling process is accomplished within time domain. Fourier

transform of the sampled signal is expressed in the following relation, as defined in (3):

$$X'(f) = \sum_{k=-\infty}^{+\infty} a_k \delta(f - \frac{k}{T_0}) \tag{3}$$

$$a_k = \frac{1}{T_0} \int_{-T_0/2}^{T_0/2} \left[ \sum_{k=0}^{N-1} x(t) \times \delta(t - k \Delta T) \right] e^{-\frac{j2k\pi}{T_0} t} dt$$

Having simplified the formula (3) and considering  $N\Delta T = T_0$ , the relation of discrete Fourier transform is expressed as (4). Therefore, the discrete Fourier transform of the signal  $x'(k\Delta t)$  will be as follows (5). But the general form of calculating the discrete Fourier transform that most of the authors use is as relation (6).

$$a_n = \sum_{k=0}^{N-1} x(k\Delta T) e^{-\frac{j2nk\pi}{N}} \quad n = 0, \pm 1, \pm 2, \dots \tag{4}$$

$$X'(\frac{n}{T_0}) = \sum_{k=0}^{N-1} x(k\Delta T) e^{-\frac{j2kn\pi}{N}} \quad n = 0, 1, 2, \dots, N-1 \tag{5}$$

$$X(r) \Big|_{t=(r-1)\Delta T} = \frac{2}{N} \sum_{k=0}^{N-1} x(r+k) e^{-\frac{2\pi}{N} jk} \quad , \quad r \geq 1 \tag{6}$$

In the above relation,  $t=(r-1) \Delta T$  is the Phasor time tag of the  $r^{\text{th}}$  sample.  $\Delta T$  is equal to  $1/f_s$ , the distance between each two sampled signals.  $N$  is the number of the samples in each sampling cycle which is specified considering the sampling frequency ( $f_s$ ) and power frequency ( $f$ )  $N = \frac{f_s}{f}$ . In the above relation,  $x(r+k)$  is also  $r+k^{\text{th}}$  sample from the sampled signal of  $x(n)$ . For example, for the first Phasor  $x(1)$  calculated at zero time, it can be written in relation (7). It should be noted that the above relation is suitable for offline applications because it uses changes in subsequent samples in the calculation of Phasor and there is no delay in following the signal changes. In real-time and immediate applications, the subsequent samples do not exist in waveform that can be used to calculate the Phasor, but the

discrete Fourier transform algorithm from the previous samples to the former cycle is used, so there is a delay of  $N\Delta T$  seconds, unless the sampling window changes in accordance with sample variation. To adapt with the actual conditions, the Phasors obtained with the labels can be delayed by  $N\Delta T$  seconds or the relation (8) can be used for real time use:

$$X(l) \Big|_{t=0} = \frac{2}{N} \sum_{k=0}^{N-1} x(1+k) e^{-\frac{j2\pi k}{N}} = \frac{2}{N} [x(1)e^{-j0} + x(2)e^{-\frac{j2\pi}{N}} + \dots + x(N)e^{-\frac{j2\pi}{N}(N-1)}] \tag{7}$$

$$X(r) \Big|_{t=(r-1)\Delta T} = \frac{2}{N} \sum_{k=0}^{N-1} x[(r-1+k-N)\Delta T] e^{\frac{2\pi}{N} jk} \quad , \quad r \geq 1 \tag{8}$$

### Clarke Transform

The three-phase lines have considerable electromagnetic coupling. In order to eliminate the coupling effect between phases and employ the modal wave method, the signals of phase domain are converted into modal component by a Modal transform. It is one of the famous transformations that has been used in this paper. The independence of these quantities makes any mode of calculation easy and is not influenced by other modes. Having used this transformation, the fault calculation can be applied in any modes and the result can be analyzed based on it. This transformation can also be applied to the three phase time waves and their Phasors, in any case, this transformation will make the input of the three-phase independent. The result is that the Clarke transformation only performs the transition from the fuzzy domain to the Modal and does not do anything per se, but for the considered purpose, other relations should be used to achieve the objectives of the problem. For example, in this paper for short circuit calculations and identifying fault phases and locating the fault, some indicators should be defined based on the voltage and current relations in the modal domain and utilize them to this end [14].

### Indicators of Fault Detection/Localization

The purpose of online detection and locating of the fault for each line of three-phase is based on the Phasor measurement techniques. The

general diagram of the comparative detecting/locating technique based on the Fourier transform is shown in Fig.1 on the basis of the equations described in this section.

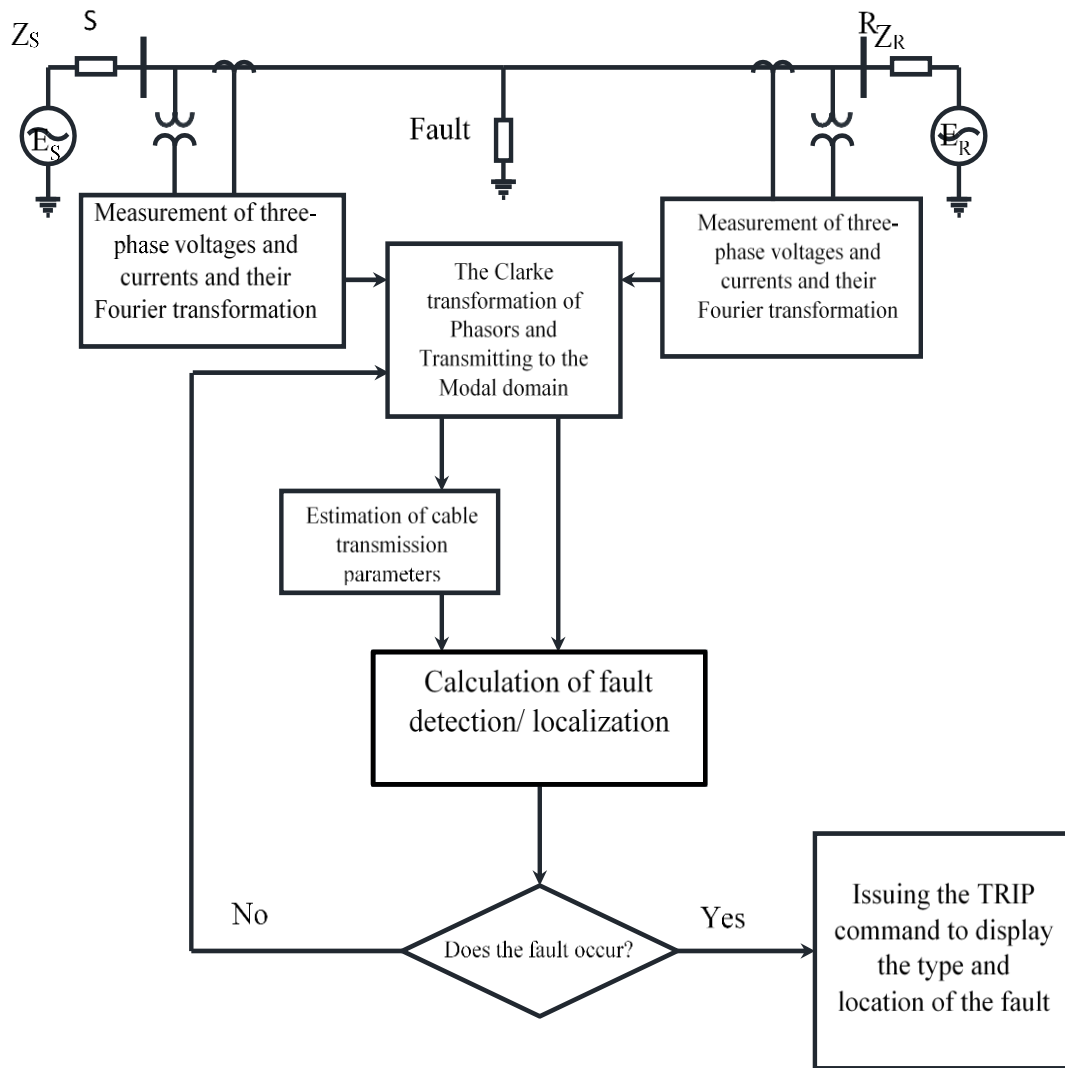


**Figure 1** The structure of the comparative detecting/locating of EHV/UHV transmission line based on the Fourier and Modal Transformations and the defining indices.

Voltage and current measurement units are installed at both ends of the line. The three-phase voltages and currents measured at both ends of the line are converted by Fourier transform into Phasoric components, the Phasors in the fuzzy domain are transmitted by the Clarke transformation into the modal domain, and on the basis of which the transmission line parameters are estimated approximately. Then, using the fault detection

and location indicators that are related to the characteristics of the line, the occurrence, the type of fault, and its location will be estimated.

### *The Simulation and Modeling of Cable Transmission Lines in the EMTP/ATP Software*

In this paper, Marti model is used for underground cables. The single-line diagram of the studied model is presented in Figure 2. The

adjacent cable network model is modeled on both sides of the S and R bus with a voltage source of  $\angle 10$  and  $230\angle 0$  kV. The characteristics of the external networks and their modeling are not considered, because the

method of using the detection and location indicators is completely independent of the type of network and depends on the Phasor voltage and the current at the two terminal ends connected to the cable.

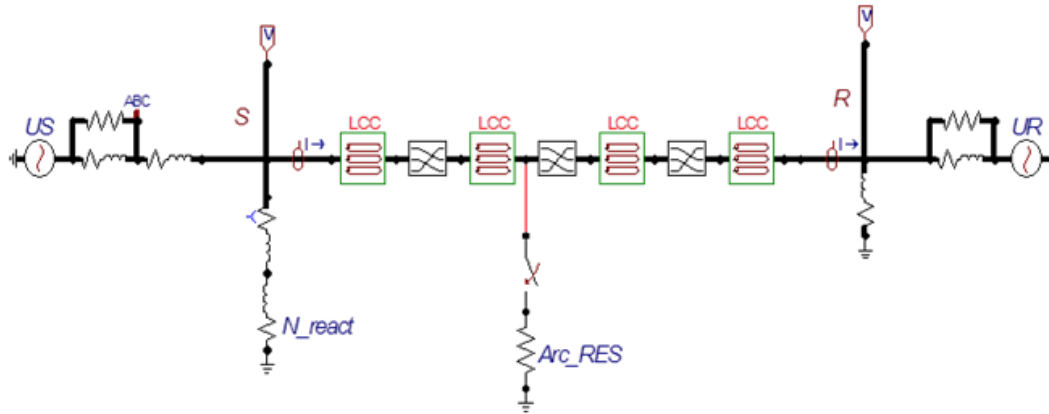


**Figure 2** The single-line diagram and infinite bus

In the studied model, the length of cable between the two networks is 40 kilometers and its rated voltage is 230kV. The physical

characteristics of the cable are also shown in Table 1.

**Table 1** The physical characteristics of XLPE cable with rated voltage of 230kV

The parameter name	Value
Inner radius of core (cm)	0.0
Outer radius of core(cm)	2.34
Inner radius of pit (cm)	3.85
Outer radius of pit (cm)	4.13
External radius of insulation (cm)	4.84
Core resistance ( $\Omega$ -m)	$0.0170 \times 10^{-8}$
Insulation resistance ( $\Omega$ -m)	$0.2100 \times 10^{-6}$
$\epsilon_r$ for inner insulation	3.5
$\epsilon_r$ for outer insulation	8.0
Relative permeability coefficient $\mu_r$	1.0
Ground resistance ( $\Omega$ -m)	100

*Comparison of the Results of Various Types of Faults*

In this section, the relevant simulation of AG and BG single-phase faults and ABG two-phase fault for 1-, 100- and 1000-ohm fault at 0.3

seconds and 0.305 seconds in different points of the cable at 50% and 25% cable length resistance at bus R is given in the respective tables and the type and locations of the calculated fault and the time and calculation faults are presented. The calculations of other

faults in different places and times can also be done and the results can be observed

**Table 2** Types of fault created in the middle of the cable and the indicators of detection and location and their diagnosis time

Time of finding the fault location with the percentage of the fault	The percent of locating fault indicator	The fault localization (kilometer)	The amount of locating fault indicator	Time of detecting the type of fault (seconds)	The performance of detection indicators of fuzzy fault	Time of fault occurrence (seconds)	Fault resistance (ohm)	Type of fault	The distance of fault from the source S
0.3262	0.0123	20.0025	0.4999	0.3006	Na, Ma(100%)	0.3	1		
0.4289	0.1611	20.0322	0.4991	0.307	Na, Ma(100%)	0.305			
0.3327	0.0234	20.0047	0.4998	0.3017	Na, Ma(100%)	0.3	100	AG	
0.3382	0.0043	20.0009	0.4999	0.3083	Na, Ma(100%)	0.305			
0.3415	0.0016	20.0003	0.4999	0.3115	Na, Ma(100%)	0.3	1000		
0.3425	0.012	20.0024	0.4999	0.3187	Na, Ma(100%)	0.305			
0.3956	-0.1688	19.9662	0.5008	0.3013	Nb, Mb(100%)	0.3	1		
0.3656	0.1847	20.0669	0.4991	0.3057	Nb, Mb(100%)	0.305			
0.3349	0.0053	20.0011	0.4999	0.3055	Nb, Mb(100%)	0.3	100	BG	20km
0.3399	0.024	20.0048	0.4999	0.3068	Nb, Mb(100%)	0.305			
0.3395	0.0361	20.0072	0.4999	0.3159	Nb, Mb(100%)	0.3	1000		
0.3439	-0.0021	19.9996	0.5000	0.3169	Nb, Mb(100%)	0.305			
0.3676	0.1661	20.0332	0.4992	0.3014	Na, Ma, Nb, Mb(100%)	0.3	1		
0.4176	-0.1555	19.9689	0.5008	0.3064	Na, Ma, Nb, Mb(100%)	0.305			
0.3316	0.0092	20.0018	0.5000	0.3024	Na, Ma, Nb, Mb(100%)	0.3	100	ABG	
0.3359	-0.0195	19.9968	0.5001	0.3017	Na, Ma, Nb, Mb(100%)	0.305			
0.3409	0.0065	20.0013	0.5000	0.3063	Na, Ma, Nb, Mb(100%)	0.3	1000		
0.3419	0.0253	20.0051	0.4999	0.3094	Na, Ma, Nb, Mb(100%)	0.305			

In Table 2, the minimum fault is related to a short-circuit AG with a resistance of 1000 ohms at 0.3 seconds, which is 0.0016%, which is 41.5 millisecond after an error occurring, equivalent to two power cycles. Of course, the delay of a cycle is related to the completion of the Fourier transformation information window completion process. Apart from AG and ABG

errors, an ohmic time of 0.305 seconds in other cases, with increasing error resistance, is observed relatively, the error location time has increased in addition to the detection time. In the case of error accuracy, the result is approximately the opposite, that is, with an increase in error resistance, the accuracy of the error also increased relatively. As can be said,

with more time spent locating, the error is reduced, and this is normal. With the observation and comparison of all the states specified in the table and their results, it is easy to determine the efficiency of using the

combined method of this dissertation. According to the above table, in the worst case, the distance between the computed error location is 36.9 meters in 40 kilometers and at best 30 cm in relation to the correct location.

**Table 3** Errors generated in 25% of cable relative to bus R and detection and location indicators and their detection time

Time of finding the fault location with the percentage of the fault	The percent of locating fault indicator	The fault localization (kilometer)	The amount of locating fault indicator	Time of detecting the type of fault (seconds)	The performance of detection indicators of fuzzy fault	Time of fault occurrence (seconds)	Fault resistance (ohm)	Type of fault	The distance of fault from the source S
0.3388	0.1042	30.0313	0.2492	0.3090	Na, Ma(100%)	0.3	1	AG	30km
0.4689	-0.1022	29.9693	0.2508	0.3069	Na, Ma(100%)	0.305			
0.3326	0.0117	30.0035	0.2499	0.3016	Na, Ma(100%)	0.3	100		
0.3391	-0.0090	29.9973	0.2501	0.3082	Na, Ma(100%)	0.305			
0.3407	0.0039	30.0012	0.2500	0.3114	Na, Ma(100%)	0.3	1000		
0.3429	0.0253	30.0076	0.2498	0.3193	Na, Ma(100%)	0.305			
0.4655	-0.0790	29.9763	0.2506	0.3018	Nb, Mb(100%)	0.3	1	BG	
0.4255	-0.1214	29.9636	0.2509	0.3059	Nb, Mb(100%)	0.305			
0.3355	0.0107	30.0032	0.2499	0.3054	Nb, Mb(100%)	0.3	100		
0.3395	0.0241	30.0072	0.2498	0.3067	Nb, Mb(100%)	0.305			
0.3389	0.0403	30.0121	0.2497	0.3158	Nb, Mb(100%)	0.3	1000		
0.3436	0.0085	30.0025	0.2499	0.3168	Nb, Mb(100%)	0.305			
0.4275	-0.1152	29.9654	0.2509	0.3012	Na, Ma, Nb, Mb(100%)	0.3	1	ABG	
0.4575	0.1231	30.0369	0.2491	0.3067	Na, Ma, Nb, Mb(100%)	0.305			
0.3368	-0.1238	29.9988	0.2500	0.3023	Na, Ma, Nb, Mb(100%)	0.3	100		
0.3366	-0.0118	29.9965	0.2501	0.3071	Na, Ma, Nb, Mb(100%)	0.305			
0.3401	0.0104	30.0031	0.2499	0.3064	Na, Ma, Nb, Mb(100%)	0.3	1000		
0.3452	0.0048	30.0015	0.2500	0.3095	Na, Ma, Nb, Mb(100%)	0.305			

In Table 3, the minimum fault of 0.9 ms, and the highest of 18.8 ms, is related to the 1000-ohm single-phase fault at 0.305 seconds. The lowest fault in the calculation of the locating

indicator is 0.009%, which is equivalent to a 2.7 cm longitudinal fault relative to 40 km. On the other hand, the highest fault in the ABG two-phase fault with a 1-ohm resistor appears at

0.305 seconds, and the fault of this indicator is 0.1231%, which is 36.9 meters. In the case of location time, the minimum time is related to the fault of the AG of 100 ohms at 0.3 seconds with a location fault of 0.0117%, which is 32.6 milliseconds, and the maximum time, as in the previous state, for an AG fault of 0.305 seconds equal to 163.9 milliseconds S is seen.

The absolute calculated values must also be calculated on the basis of the length of the short line, which the reference articles [7-9] does not

specify the total length of the power cable, although the magnitude of the fault of location is based on the percentage of comparison and is important. It is clear from Table 4 that the short-circuit location fault in this thesis is far less than references [8] and expresses the superiority of the method proposed in this paper to other methods such as wavelet transform. Meanwhile, the time and type of fault, and the total length of the cable, are not included in this reference.

**Table 4.** Evaluation of the proposed method than other methods

Method	The percent of fault	The fault location
Wavelet transform	4.48	512
Fit curve	3.36	508
The proposed method of the article	3.26	506

## Conclusion

In this paper, the use of Fourier transforms as a powerful tool in obtaining the size and angle of each phase is proposed, which obtains complete information on voltage parameters and power grid flows. An online approach is proposed using Fourier transform data on both sides of a cable line that uses detection and location indicators in both the modal and fuzzy domains, and its excellent utilization is shown. The use of Clarke transformation and transition to the modal domain for the independence of the components used to study a variety of studies including fault has been proposed which in addition to reducing the volume of equations caused by the dependence between fuzzy components, it also increases the degree of assurance of the accuracy of the results. The delay of fault detection and location indicators is very negligible and limited to the delay caused by the Fourier transform calculations. In addition, the accuracy of the calculations of these indicators is very high, and in this case, most of the fault is due to the essence of the Fourier transformation. The responses of fault detection indicators in the modal and even fuzzy domains are also correct in 100% of cases. The maximum computational fault caused by the fault location indicator in the modal domain was less than 5.0%. The

precision of the proposed hybrid approach is more than just a number of methods, such as wavelet transform.

## ORCID

Ebadollah Amouzad Mahdiraji  
<https://orcid.org/0000-0003-3777-4811>

## References

- [1] K.K. Kuan, K. Warwick, *IEE Proceedings C: Generation, Transmission and Distribution*, **1992**, *139*, 235-240. [[crossref](#)], [[Google Scholar](#)], [[Publisher](#)]
- [2] E.A. Mahdiraji, N. Ramezani, *2015 2nd International Conference on Knowledge-Based Engineering and Innovation (KBEI)*, Tehran, Iran, **2015**, 405-411. [[crossref](#)], [[Google Scholar](#)], [[Publisher](#)]
- [3] E.A. Mahdiraji, M.S. Amiri. *International Journal of Smart Electrical Engineering*, **2020**, *9*, 13-21. [[Google Scholar](#)], [[Publisher](#)]
- [4] E.A. Mahdiraji, M. Amiri, *Journal of Engineering Technology and Applied Sciences*. **2020**, *5*, 133-147. [[crossref](#)], [[Google Scholar](#)], [[Publisher](#)]
- [5] M.M.A. Aziz, E.S.T. El Din, D.K.L Ibrahim, M. Gilany, *Electric Power Components and*

- Systems*, **2006**, *34*, 417–432. [[crossref](#)], [[Google Scholar](#)], [[Publisher](#)]
- [6] X. Yang, M.S. Choi, S.J. Lee, C.W. Ten, S.I. Lim, *IEEE Trans.Power System*, **2008**, *23*, 1809-1816, [[crossref](#)], [[Google Scholar](#)], [[Publisher](#)]
- [7] E.S.T.E. Din, M. Gilany, M.A. Aziz, D.K. Ibrahim, *Power Engineering Society General Meeting, 2005. IEEE*, **2005**, *1*, 80–86. [[crossref](#)], [[Google Scholar](#)], [[Publisher](#)]
- [8] E.T. El Din, M. Gilany, M.A. Aziz, D.K. Ibrahim, *Power Engineering Society General Meeting, 2005. IEEE*, **2005**, *3*, 2485–2491. [[crossref](#)], [[Google Scholar](#)], [[Publisher](#)]
- [9] K. Ming-Cai, W. Yang, Z. Jun-Fang, H. Guang, Y. Qiu, *Sustainable Power Generation and Supply (SUPERGEN 2012), International Conference on*, **2012**, 1–6. [[crossref](#)], [[Google Scholar](#)], [[Publisher](#)]